Direct Orthotopic Implantation of Hepatic Organoids

Vivian X. Zhou, BA[a], **Macarena Lolas, MD, PhD**[a], and **Tammy T. Chang, MD, PhD**[a,b]

[a]Department of Surgery, University of California, San Francisco, 513 Parnassus Avenue, San Francisco, CA 94143

[b]Liver Center, University of California, San Francisco, 513 Parnassus Avenue, San Francisco, CA 94143

Abstract

Background—Liver organoids show promise for development as a tissue replacement therapy for patients with end-stage liver disease, but efficient methods for introducing organoids into host livers have not been established. In this study, we aimed to develop a surgical technique to implant hepatic organoids into the liver and assess their engraftment.

Methods—Donor hepatocytes were isolated from ROSA26 C57BL/6 mice so that engrafted cells, when implanted into wild-type mice, could be easily identified by Xgal staining. Hepatic organoids were generated by three-dimensional culture in rotating wall vessel bioreactors. We qualitatively and quantitatively compared organoid engraftment to that of single-cell hepatocyte transplants. In addition, we determined the effect of adding stellate cells to hepatocytes to form co-aggregated organoids and the effect of partial hepatectomy of the host liver on organoid engraftment.

Results—Direct orthotopic implantation of hepatic organoids within a hepatotomy site resulted in local engraftment of exogenous hepatocytes with limited durability. Hepatocyte-stellate cell organoids produced more extracellular matrix but did not significantly improve engraftment compared to hepatocyte-alone organoids. Partial hepatectomy of the host liver led to significantly decreased engraftment of organoids. Survival of organoids was limited by the presence of apoptotic hepatocytes within organoids as early as 1 hour after implantation. Organoids eventually became necrotic and elicited a chronic inflammatory giant cell reaction similar to a foreign body response.

Conclusion—With additional organoid and host factor optimization, direct orthotopic implantation of hepatic organoids may be an approach to introduce large numbers of exogenous hepatocytes into recipient livers.

Keywords

Introduction

Organoids are three-dimensional (3D) aggregates of organ-specific cells that self-organize *in vitro* into *in vivo*-like tissue structures. Recent advances have led to the generation of retinal, brain, kidney, gut, and liver organoids that recapitulate some of the specific functions of those organs. Importantly, organoids have great therapeutic potential if effective implantation strategies can be developed for organoids to replace diseased or dysfunctional organs in humans.[1]

Liver transplantation is currently the only treatment for end-stage liver disease, which is the 12th leading cause of death by disease in the United States.[2] Transplantation is limited by the severe shortage of donor organs and there is a critical need to develop alternative approaches to replace lost liver function. Human liver organoids have been developed from induced pluripotent stem cells[3] and adult bipotential liver stem cells[4] by culturing in extracellular matrix (ECM) produced by Engelbreth-Holm-Swarm mouse sarcoma cells (marketed under the tradename Matrigel). While initial efforts to implant liver organoids into mouse models showed promising results, they remain limited in that either engraftment sites were ectopic (e.g. brain, kidney capsule, or mesentery)[3] or engraftment efficiency into the liver was low.[4] In addition, engraftment required genetically engineered mouse models[3, 5] or pre-treatment with toxins[4] that conferred a proliferative advantage to implanted cells over endogenous hepatocytes, conditions that could not be recapitulated easily clinically. Implantation experiments were conducted in severely immunodeficient mice[3–5] and likely do not reflect the immunological reaction that would be elicited in a clinical scenario in humans. Finally, dependence on Matrigel for organoid formation is problematic because Matrigel is a collection of undefined protein products from a xenogenic source that cannot easily be translated into clinical applications.

Our lab has generated liver organoids in rotating wall vessel (RWV) bioreactors that provide an unencumbered 3D spatial environment for cells to self-aggregate and self-organize.[6, 7] This approach has the advantage of efficiently producing bulk cultures of organoids that initiate cellular self-organization in a 3D environment, as opposed to Matrigel-based methods that coax development of 3D structures from a two-dimensional (2D) surface. Moreover, formation of organoids in RWVs does not rely on Matrigel. RWVs produce solid-body rotation with laminar flow, resulting in an idealized suspension culture with low turbulence, low shear stress, and maximal 3D spatial freedom for cells to self-associate.[8] These unique features promote formation of larger aggregates that have decreased hypoxia near the core compared to stationary methods.[9] Organoids that mimic the *in vivo* architecture of numerous organs, including lung, intestine, bladder, and liver, have been

successfully generated in RWVs.[10] Hepatocytes that self-aggregate within RWVs form tight junctions and bile canaliculi[11] and display differentiated characteristics that make them good models to study hepatitis C host-pathogen interactions.[12] Our lab has shown that compared to 2D culture, hepatic organoids generated in RWVs have significantly greater hepatocyte-specific functions and gene expression because of maintained expression of a key master transcriptional regulator, hepatocyte nuclear factor 4 alpha.[6, 7]

In this study, we aimed to develop a surgical technique to orthotopically implant hepatic organoids generated within RWVs into the livers of recipient mice. Achieving orthotopic implantation is important because full expression of critical hepatic functions, including bile excretion and processing of portal circulation metabolites, requires engraftment in the unique anatomical location of the liver. We hypothesized that hepatocyte organoids generated in RWVs would produce their own ECM and that the ECM scaffold would be further enhanced by co-culture with stellate cells. We used immunocompetent mice as recipients to determine if our surgical approach stimulated immune responses that limited the durability of engraftment. Finally, novel surgical approaches, including associating liver partition and portal vein ligation for staged hepatectomy (ALPPS), indicate that hepatectomy may be used therapeutically to induce rapid hypertrophy of the remnant liver.[13] Therefore, we tested the effect of performing partial hepatectomy on the recipient liver at the time of organoid implantation as a clinically translatable surgical adjunct to promote organoid engraftment.

Methods

Mice

B6.129S7-Gt(ROSA)26Sor/J (ROSA26) mice (6–12 weeks old), in which β-galactosidase was constitutively expressed in all cells, were maintained as a colony in-house. Male or female ROSA26 mice were used as sources of donor hepatocytes and stellate cells. Male wild-type littermates or wild-type C57BL/6 mice purchased from Jackson Laboratory (Bar Harbor, ME) were used as recipient mice in implantation experiments. All mice were cared for in accordance to the National Institutes of Health "Guide for the Care and Use of Laboratory Animals."

Generation of Liver Organoids

Primary hepatocytes were isolated by two-step perfusion using Liver Perfusion Medium and Liver Digest Medium (Thermo Scientific, Fremont, CA), and then separated with 50% Percoll (GE Healthcare Life Sciences, Pittsburgh, PA) density gradient. Primary stellate cells were isolated by three-step perfusion using Liver Perfusion Medium (Thermo Scientific), 0.29% pronase (Roche, Basel, Switzerland), and 0.024% collagenase (Crescent Chemical, Islandia, NY), followed by further digestion in 0.044% pronase and 0.008% DNase (Roche). Stellate cells were then separated by a 15.6%/8.5% Accudenz (Accurate Chemical, Westbury, NY) density gradient at 20,000 rpm in an Optima LE-80K ultracentrifuge rotor 5519 (Beckman Coulter, Brea, CA). Hepatocytes alone or hepatocytes with stellate cells at a 10:1 ratio were placed in Dulbecco's modified Eagle's medium supplemented with 5% fetal calf serum (Hyclone, Logan, UT), L-glutamine, antibiotics, insulin-transferrin-selenium, and

HEPES (Mediatech, Manassas, VA) at a final density of 1×10^5 cells/ml. Organoids were formed by self-association by culturing for 3 days in high-aspect-ratio-vessel RWVs with 50mL capacity (Synthecon, Houston, TX) at a rotation speed of 12rpm. The viability of organoids was confirmed by the trypan blue exclusion test in which they were stained with 0.4% trypan blue (Sigma, St. Louis, MO) diluted 1:9 in phosphate buffered saline and wet-mounted onto a slide. Bright-field photos were taken with a Canon EOS Rebel T3i (Canon, Tokyo, Japan) adapted to the photoport of a Nikon Eclipse TS100 microscope (Nikon, Tokyo, Japan).

Orthotopic Liver Organoid Implantation

Liver organoids were collected from RWVs, counted, and resuspended in phosphate buffered saline. PE50 tubing (BD Biosciences, San Jose, CA) was loaded with 1,000 organoids (approximately 1×10^6 cells) and adapted to a glass syringe with screw drive (Hamilton, Reno, NV). For direct orthotopic implantation, a hepatotomy was made in the left liver lobe of recipient mice using a 16-gauge needle, and the organoids were then implanted within the hepatotomy site. For comparison, 1×10^6 freshly isolated single-cell hepatocytes were loaded into PE50 tubing and implanted into the left lobe in the same manner. In some recipient mice, concurrent two-thirds hepatectomy was carried out by ligating and resecting the median and left lobes, followed by a hepatotomy and organoid implantation in the remaining right liver lobe. Single-cell hepatocytes were injected into the spleen using a 30-gauge needle and organoids were infused into the spleen with PE50 tubing. Anesthesia, aseptic technique, perioperative care, and analgesia were performed in accordance to standard procedures and protocols approved by the Institutional Animal Care and Use Committee at UCSF. Recipient mice were sacrificed 1 hour, 3 days, or 7 days after organoid implantation and their livers collected for analysis.

Histology

Livers were fixed for 5 hours in periodate-lysine-paraformaldehyde solution, which consisted of 0.2% sodium phosphate monobasic monohydrate (Fisher Scientific, Hampton, NH), 1.6% sodium phosphate dibasic heptahydrate (Fisher Scientific), 1% lysine (Sigma), 2% paraformaldehyde (Alfa Aesar, Haverhill, MA), and 0.22% sodium periodate (G-Biosciences, St. Louis, MO) at pH 7.4. Livers were then dehydrated in 30% sucrose (Sigma) overnight, embedded in OCT compound (Sakura, Torrance, CA), frozen via contact with dry ice, and cut into 10 μm sections using a Leica CM3050 S cryostat (Leica Biosystems, Buffalo Grove, IL). Liver sections were incubated in a solution consisting of 0.015% magnesium chloride (Sigma), 0.13% potassium ferricyanide (Ward's Science, Rochester, NY), 0.17% potassium ferrocyanide (Chem Service, West Chester, PA), and 0.08% 5-bromo-4-chloro-3-indolyl-β-D-galactopyranoside (Xgal; Teknova, Hollister, CA) overnight to stain for engrafted cells. Sections were then counterstained with hematoxylin (Ricca Chemical, Arlington, TX) and eosin (Electron Microscopy Sciences, Hatfield, PA) using standard procedures and mounted using Permount (Fisher Scientific). Bright-field photos were taken with a Zeiss Axiocam MRc 5 adapted to the photoport of a Zeiss Axiostar Plus microscope (Zeiss, Oberkochen, Germany).

Analysis of Organoid Engraftment

Liver section images were digitally acquired and processed by ImageJ software (Bethesda, MD). Measurements were taken from sections with the largest cross-sectional area of implanted hepatocytes from a total cryosectional depth of 600 μm. Implanted hepatocytes in each section were quantified by converting the images to 8-bit and then applying a threshold of 0–2.5% to select only the darker, blue donor cells over the lighter, pink host tissue. Hepatocyte aggregates were segmented into individual cells using the binary/watershed function. Particle analysis was then used to count the number of donor hepatocytes in each image, using parameters of 70-infinity cm^2 (size) and 0.00–1.00 (circularity) to ignore any small non-hepatocyte cells or debris.

Immunofluorescence Confocal Microscopy

Whole mount staining was performed on liver organoid samples that were fixed in 4% paraformaldehyde, permeabilized with 0.1% Triton X-100 (Promega, Madison, WI) in phosphate buffered saline, and blocked in 10% goat serum (Jackson ImmunoResearch Laboratories, West Grove, PA). Samples were incubated with the following primary antibodies at 4°C overnight: anti-collagen I (1:200, ab21286; Abcam, Cambridge, MA), anti-collagen IV (1:200, ab6586; Abcam), anti-laminin (1:30, L9393; Sigma), anti-fibronectin (1:100, ab2413; Abcam), anti-desmin (1:200, RB-9014-P0; Thermo Scientific), and anti-alpha smooth muscle actin (1:200, ab21027; Abcam). Signal detection was achieved with secondary antibodies AlexaFluor-488-conjugated goat anti-rabbit IgG or donkey anti-goat IgG (1:500; Jackson InmmunoResearch, West Grove, PA). F-actin was visualized with AlexaFluor-488 phalloidin (Thermo Scientific) and nuclei were counterstained with l μg/ml 4'6-diamidino-2-phenylindole (DAPI). In some experiments, stellate cells were pretreated with CellTracker Red CMTPX dye (Thermo Scientific) prior to culture. Samples were imaged using a Yokagawa CSU22 spinning disk confocal microscope at the UCSF Nikon Imaging Center (San Francisco, CA).

Quantification of Organoid ECM

Using Image J software, we analyzed confocal images of organoids by converting positive staining for each matrix component into binary mode through the histogram threshold function, followed by particle analysis. To calculate the percentage area positive for a specific matrix component, the area positive for that matrix obtained from particle analysis was divided by the cross-sectional area of the entire organoid, which was determined by the tracing tool. This analysis was performed for at least 10 organoids for each matrix component for each condition.

Terminal deoxynucleotidyl transferase (TdT) dUTP nick-end labeling (TUNEL)

TUNEL staining was performed on liver cryosections using the ApopTag Peroxidase In Situ Apoptosis Detection Kit (Millipore, Billerica, MA) per manufacturer's instructions. Viable nuclei were detected by counterstaining with methyl green (Sigma).

Statistical Analysis

Statistical analyses were performed with Prism v. 5.0 (GraphPad, La Jolla, CA) using either Student's two-tailed t-test or two-way ANOVA. P values < 0.05 were considered statistically significant.

Results

Direct orthotopic implantation of hepatocyte organoids results in local engraftment of organoids into the implanted liver lobe

To evaluate the engraftment potential of liver organoids generated in RWVs, we isolated primary hepatocytes from ROSA26 C57BL/6 mice, whose cells express β-galactosidase under a ubiquitous promoter and stain blue in the presence of Xgal. Hepatocytes self-organized into organoids 100–200μm in size within 3 days of culture in RWVs.[7] Conventional clinical and experimental hepatocyte transplantation entails injecting hepatocytes into the portal circulation through the portal vein or via the spleen. We found that injection of donor Xgal[+] hepatocytes into recipient spleens resulted in low-efficiency engraftment near portal veins of portal triads within the liver parenchyma (Figure 1A), a result consistent with published reports.[14] Rare Xgal[+] hepatocytes were detected in the spleen up to 3 days after injection, indicating that some donor hepatocytes were retained in the spleen. When we infused hepatic organoids into the spleen, we saw no engraftment of organoids in the liver after 3 days. Clusters of organoids were trapped within the spleen after splenic injection (Figure 1A), indicating that organoids were not able leave the spleen, likely due to their larger size and cohesive multicellular structure. We attempted to inject the organoids through the portal vein, however, this was too technically challenging due to the small size of the mouse portal vein.

Because organoids could not be transplanted into the liver via splenic injection, we developed a surgical technique to directly implant the organoids into the liver orthotopically. First, a hepatotomy was performed using a 16-gauge needle in the recipient liver parenchyma. Liver organoids were then infused into the hepatotomy site in a slow and controlled manner, using PE50 tubing adapted to a screw-drive glass syringe in a technique modified from murine pancreatic islet transplantation.[15] Using this surgical approach, we achieved consistently high implantation rates of liver organoids as determined by the presence of Xgal^{+} cells in recipient livers after 3 days (Figure 1B). As a comparison, we implanted freshly isolated single-cell hepatocytes into the liver parenchyma using the same technique. Single cells appeared to be loosely dispersed within the hepatotomy site, whereas organoids retained their aggregated spheroid architecture and were more compacted within the space (Figure 1B). The numbers of Xgal[+] donor hepatocytes delivered by direct parenchymal implantation were comparable whether hepatocytes were implanted as single cells or as organoids (Figure 1C). These results indicate that although organoids could not be transplanted into the liver via splenic injection, they could be implanted into the liver by direct parenchymal implantation. Orthotopic organoid implantation achieves implantation rates comparable to those of single-cell hepatocytes implanted by the same technique.

Hepatocyte-stellate cell organoids demonstrate greater ECM production compared to hepatocyte-alone organoids

Because hepatic stellate cells are the main producers of ECM in the liver,[16] we hypothesized that co-culturing hepatocytes with stellate cells would generate organoids with optimized ECM scaffolds, potentially leading to improved engraftment in host tissue. To generate hepatocyte-stellate cell organoids, we isolated primary hepatocytes and stellate cells from ROSA26 C57BL/6 mice and co-cultured them within RWVs for 3 days at a 10:1 ratio, the normal hepatocyte to stellate cell ratio within the liver. Isolated stellate cells were treated with CellTracker Red CMTPX dye so that they could be identified within hepatocyte-stellate cell organoids. Confocal microscopy demonstrated that hepatocytes had cortical organization of F-actin and that stellate cell distribution was widespread and uniform among hepatocytes in co-aggregated organoids generated within RWVs (Figure 2A). Within co-aggregated organoids, we detected quiescent stellate cells, which stain positively for desmin and exhibit a round cell shape, as well as activated stellate cells, which stain positively for alpha smooth muscle actin (αSMA) and exhibit an elongated cell shape (Figure 2B).

To determine whether hepatocyte-stellate cell organoids produced more ECM compared to hepatocyte-alone organoids, we stained both organoid types for the four major ECM components found in normal liver: collagen I, collagen IV, laminin, and fibronectin. Positive staining for each ECM component was determined by confocal microscopy and quantitatively evaluated by digital imaging analysis. In hepatocyte-stellate cell organoids, distribution of collagen I, collagen IV, and laminin increased significantly compared to hepatocyte-alone organoids, whereas fibronectin levels were similar between the two organoid types (Figure 3A and 3B). These results are consistent with the roles of stellate cells producing collagen I, collagen IV, and laminin and hepatocytes producing mostly fibronectin within the normal liver,[16] and suggest that hepatocyte-stellate cell organoids demonstrate a more complete ECM scaffold than do hepatocyte-alone organoids.

Hepatocyte-stellate cell organoids show engraftment comparable to that of hepatocyte-alone organoids, whereas partial hepatectomy of the host liver significantly decreases organoid engraftment

To determine whether the improved ECM scaffold of hepatocyte-stellate cell organoids led to improved engraftment, we implanted ROSA26 C57BL/6 hepatocyte-stellate cell and hepatocyte-alone organoids into the liver parenchyma of wild-type C57BL/6 mice. Recipient livers were collected 3 days later and stained with Xgal to identify implanted organoids. There were no qualitative differences between implantation of the two types of organoids because neither condition demonstrated integration of donor cells with the surrounding host parenchyma (Figure 4A). In addition, there were no quantitatively significant differences between the numbers of Xgal^{+} cells detected after hepatocyte-alone versus hepatocyte-stellate cell organoid implantation (Figure 4B). These results indicate that the presence of stellate cells in co-aggregated organoids results in greater ECM production, but does not significantly increase engraftment efficiency.

Since partial hepatectomy stimulated liver regeneration, we hypothesized that performing a two-thirds partial hepatectomy at the time of implantation would induce host liver tissue

remodeling and improve organoid integration with the host liver. We implanted hepatocyte-alone or hepatocyte-stellate cell organoids into recipient mice that either did or did not undergo simultaneous two-thirds hepatectomy of their remaining liver. After 3 days, partial hepatectomy led to expected hypertrophy of the remaining lobes of the host liver, but did not qualitatively improve organoid integration with host parenchyma (Figure 4A). Partial hepatectomy resulted in significantly decreased numbers of Xgal^{+} cells detected at the implantation site (Figure 4B), suggesting that host liver regeneration and tissue remodeling decreased engraftment of the organoids.

Neutrophilic infiltration around implanted organoids correlated with early apoptosis of donor hepatocytes and evolved into a chronic inflammatory reaction with multinucleated giant cells

To further investigate host and organoid factors that significantly impact organoid engraftment, we analyzed the host inflammatory response to orthotopic organoid implantation at 1 hour, 3 days, and 7 days. Immediately after implantation, a few host inflammatory cells were found around the implanted organoids. At 3 days after implantation, the number of inflammatory cells around organoids significantly increased, and by 7 days, a broad layer of inflammatory cells surrounded the organoids (Figure 5A). Quantitative analysis revealed that the number of Xgal^{+} cells within implantation sites decreased between 3 days and 7 days, suggesting limited durability of organoid engraftment (Figure 5B). Detailed morphological examination of the inflammatory infiltrate demonstrated that neutrophils were the predominant cell type infiltrating between organoids at 1 hour after implantation, consistent with an acute inflammatory response stimulated by tissue injury (Figure 5C). By day 3, the inflammatory response had matured, with recruitment of additional neutrophils, eosinophils, macrophages, and rare lymphocytes. By day 7, there were features of chronic inflammation with numerous multinucleated giant cells surrounding the remaining organoids, similar to a foreign body reaction.

To temporally correlate organoid viability with the elicited inflammatory response, we first confirmed the viability of the organoids prior to transplantation by trypan blue exclusion. The vast majority of cells within organoids were viable and excluded trypan blue (Figure 6A). In contrast, hepatocytes that remained as single cells within the RWVs were all dead and trypan blue positive, indicating that cell-to-cell contact and cellular aggregation were critical to maintaining the viability of hepatocytes in rotational suspension culture. We implanted viable hepatocyte organoids orthotopically into the liver of recipient mice and performed terminal deoxynucleotidyl transferase (TdT) dUTP nick-end labeling (TUNEL) staining to detect apoptotic cells at 1 hour and 3 days after implantation. We found that along with many viable appearing hepatocyte nuclei, a substantial number of donor hepatocytes within organoids were already TUNEL[+] as early as 1 hour after implantation (Figure 6B). By day 3, there were no viable hepatocyte nuclei within organoids. Although some hepatocytes demonstrated TUNEL[+] nuclei, most were anucleated with washed-out cytoplasm, consistent with coagulative necrosis. These results indicated that while implanted organoids continued to express Xgal at 3 days after implantation, their viability was severely compromised. In order to determine whether the site of implantation influenced the onset the organoid necrosis, we performed TUNEL staining on organoids implanted into the spleen.

Similar to the liver, organoids implanted into the spleen displayed a mix of healthy and apoptotic nuclei at 1 hour and all organoids were necrotic by 3 days (Figure 6B). Freshly isolated single-cell hepatocytes implanted into the liver by the same technique showed more viable cells at 1 hour compared to organoid implantation. However, by day 3, single-cell hepatocytes within the main implantation cavity were also necrotic (Figure 6B). These results suggest that organoids are more susceptible to early cell death after parenchymal implantation compared single-cells, but by 3 days, both organoids and single-cells, regardless of site of implantation, succumb to necrosis.

Discussion

The technology for producing highly functional liver organoids is developing rapidly, but effective techniques for engrafting them *in vivo* for therapeutic organ function replacement is lacking. Conventional single-cell hepatocyte transplantation through the portal circulation has been shown in human clinical trials to have poor engraftment efficiency, durability, and outcomes.[14] The reasons for this include clearance by the immune system and entrapment within hepatic sinusoids. We developed a novel surgical method for introducing liver organoids orthotopically into recipient liver parenchyma by performing a hepatotomy and then implanting organoids directly. We showed that attempts to introduce hepatic organoids into the portal circulation by injecting them into the spleen resulted in the organoids being trapped within the spleen, likely because they are larger than single cells and have a cohesive multicellular structure. Our surgical approach of orthotopic liver organoid implantation is conceptually innovative in that we bypass the requirement for cells to extravasate across portal sinusoids to reach and engraft within the liver.

We demonstrated that hepatocyte organoids generated in RWVs by self-organization produced their own endogenous ECM, and additional ECM was produced in organoids formed by co-culture with stellate cells. Organoid ECM composition recapitulated the *in vivo* characteristics of hepatocytes, producing mostly fibronectin, and of stellate cells, producing collagen I, collagen IV, and laminin.[16] Quiescent stellate cells play a key role in maintaining ECM homeostasis in the normal liver,[16] and our findings suggest that their presence within liver organoids may be important in maintaining a normal ECM scaffold. Stellate cell activation is required for repairing liver injury and inducing liver regeneration,[17] but continued pathological activation of stellate cells leads to fibrosis and liver dysfunction.[18] Hepatocytes and stellate cells are closely positioned in the Space of Disse *in vivo* and they cross-regulate each other through paracrine signals.[19] Insulin-like growth factor 1 produced by injured hepatocytes stimulates proliferation of stellate cells,[20] whereas hepatocyte growth factor produced by stellate cells stimulates hepatocyte proliferation and is the key mitogen in liver regeneration.[21] Co-culture experiments have demonstrated that both quiescent and activated stellate cells improve and prolong hepatocyte function *in vitro* compared to hepatocyte monoculture.[22–25] We found that both quiescent and activated stellate cells were present in hepatocyte-stellate cell organoids generated in RWVs. Although total ECM content and the diversity of ECM components were increased in hepatocyte-stellate organoids compared to hepatocyte-alone organoids, this difference did not lead to significant improvements in organoid engraftment, suggesting that the

composition of organoid ECM scaffolds was not a key determinant of successful engraftment.

Studies to date have investigated liver organoid engraftment in experimental models in which host hepatocytes were manipulated to give transplanted cells a growth advantage. These experimental systems utilized genetically engineered mouse models, such as fumarylacetoacetate hydrolase deficient mice[5] or albumin thymidine kinase transgenic mice,[3] in which specific forms of host hepatocyte injury were induced to facilitate endogenous hepatocyte replacement by exogenously introduced hepatocytes. These studies demonstrated the functional capacity of engrafted liver organoids *in vivo*, but the experimental conditions favorable for engraftment had limited or no human correlate for clinical translation. Another study used carbon tetrachloride and retrorsine to pre-condition the host livers of mice for organoid engraftment,[4] but the safety and efficacy of those toxins in humans were unknown. Recent advances in surgery indicate that hepatectomy may be used therapeutically to induce hypertrophy in the remnant liver and permit extensive resection of liver tumors.[13] We hypothesized that hepatectomy may be used to induce improved engraftment and/or proliferation of orthotopically implanted liver organoids. We found that although two-thirds hepatectomy induced the expected hypertrophy of the remnant host liver, it did not qualitatively improve integration of implanted organoids with the host parenchyma and quantitatively decreased the number of engrafted donor cells. These results suggested that the regenerative signals induced by hepatectomy did not reach the organoids and have a chance to stimulate beneficial proliferative effects, possibly because of limited organoid viability and the inflammatory reaction that surrounded the organoids. Instead, tissue hypertrophy and remodeling induced by hepatectomy may have sped up the elimination of organoids by the inflammatory infiltrate. Our results illustrate that developing strategies to introduce exogenous hepatocytes into the liver remains an important challenge. Single-cell hepatocyte transplantation through the portal vein produces less acute inflammation, but engraftment efficiency is low due to entrapment of donor cells within sinusoids and clearance by the reticulo-endothelial system.[14] Efficient transplantation of organoids through the portal system may be even more challenging due to their larger size and multi-cellular structure. Additional innovation is required to facilitate engraftment of exogenous hepatocytes or organoids into the liver and need to address the inflammatory/immunological response.

Our analysis showed that at 1 hour after implantation, there was neutrophilic infiltration around the organoids, consistent with a response to acute tissue injury. At this same time point, a substantial number of donor hepatocytes within organoids had TUNEL[+] nuclei, indicating that they were undergoing apoptosis. Our surgical technique of direct parenchymal implantation produced traumatic tissue injury to the host liver that likely stimulated a neutrophil response. In addition, another source of tissue injury at the implantation site might have been ischemia-reperfusion injury of the organoids. Ischemia-reperfusion injury is an important cause of organ dysfunction after major liver resections and liver transplantation.[26] Liver organoids may have experienced ischemia-reperfusion as a consequence of transfer from the bioreactor followed by subsequent reperfusion by blood released from disrupted sinusoids at the implantation site. Our data showed that viability of single-cells was better than organoids at 1 hour after implantation, suggesting that organoids

may be more vulnerable to ischemia. Parenchymal cells in the liver and intestine undergo apoptosis 1 hour after reperfusion in experimental transplantation models,[27, 28] a time course similar to the onset of hepatocyte apoptosis in implanted organoids. Eventually, the dominant mode of cell death after ischemia-reperfusion injury was necrosis,[28] also similar to what we observed after organoid implantation. Ischemia-reperfusion injury is characterized by induction of oxidative stress, parenchymal cell apoptosis, and immune activation.[26] Our findings suggest that for orthotopic liver organoid implantation to succeed clinically, the acute inflammatory response induced by tissue injury from the implantation procedure, and potentially from ischemia-reperfusion, must be minimized. Various approaches aimed at reducing the inflammatory consequences of tissue injury are currently under investigation, including pre-operative conditioning, administration of anti-oxidants, nitric oxide agonists, anti-apoptotic and anti-inflammatory agents.[29, 30] Novel immunomodulatory agents that inhibit natural IgM antibodies and complement activation have also been shown to dampen the acute inflammation caused by tissue injury.[31, 32] Our data suggest that these novel approaches to reduce acute inflammation will likely be important adjuncts to improve the efficiency and durability of orthotopic liver organoid implantation.

In conclusion, liver organoids generated in RWVs produced endogenous ECM scaffolds and could be further developed for *in vivo* tissue replacement therapy for patients with end-stage liver disease. Further optimization of clinically modifiable organoid and host factors are needed to improve the durability of orthotopic liver organoid engraftment.

Acknowledgments

Abbreviations

3D	three-dimensional
2D	two-dimensional
RWV	rotating wall vessel
ECM	extracellular matrix
H&E	hematoxylin and eosin
αSMA	alpha smooth muscle actin
TUNEL	terminal deoxynucleotidyl transferase (TdT) dUTP nick-end labeling

References

1. Lancaster MA, Knoblich JA. Organogenesis in a dish: modeling development and disease using organoid technologies. Science. 2014; 345:1247125. [PubMed: 25035496]

2. 12/2/2014 ed: Centers for Disease Control and Prevention. 2015. Deaths, Percent of Total Deaths, and Death Rates for the 15 Leading Causes of Death: United States and Each State, 1999–2013.

3. Takebe T, Sekine K, Enomura M, Koike H, Kimura M, Ogaeri T, et al. Vascularized and functional human liver from an iPSC-derived organ bud transplant. Nature. 2013; 499:481–484. [PubMed: 23823721]

4. Huch M, Gehart H, van Boxtel R, Hamer K, Blokzijl F, Verstegen MM, et al. Long-term culture of genome-stable bipotent stem cells from adult human liver. Cell. 2015; 160:299–312. [PubMed: 25533785]

5. Huch M, Dorrell C, Boj SF, van Es JH, Li VS, van de Wetering M, et al. In vitro expansion of single Lgr5+ liver stem cells induced by Wnt-driven regeneration. Nature. 2013; 494:247–250. [PubMed: 23354049]

6. Chang TT, Hughes-Fulford M. Monolayer and spheroid culture of human liver hepatocellular carcinoma cell line cells demonstrate distinct global gene expression patterns and functional phenotypes. Tissue Eng Part A. 2009; 15:559–567. [PubMed: 18724832]

7. Chang TT, Hughes-Fulford M. Molecular mechanisms underlying the enhanced functions of three-dimensional hepatocyte aggregates. Biomaterials. 2014; 35:2162–2171. [PubMed: 24332390]

8. Hammond TG, Hammond JM. Optimized suspension culture: the rotating-wall vessel. Am J Physiol Renal Physiol. 2001; 281:F12–F25. [PubMed: 11399642]

9. Curcio E, Salerno S, Barbieri G, De Bartolo L, Drioli E, Bader A. Mass transfer and metabolic reactions in hepatocyte spheroids cultured in rotating wall gas-permeable membrane system. Biomaterials. 2007; 28:5487–5497. [PubMed: 17881050]

10. Barrila J, Radtke AL, Crabbe A, Sarker SF, Herbst-Kralovetz MM, Ott CM, et al. Organotypic 3D cell culture models: using the rotating wall vessel to study host-pathogen interactions. Nat Rev Microbiol. 2010; 8:791–801. [PubMed: 20948552]

11. Khaoustov VI, Darlington GJ, Soriano HE, Krishnan B, Risin D, Pellis NR, et al. Induction of three-dimensional assembly of human liver cells by simulated microgravity. In Vitro Cell Dev Biol Anim. 1999; 35:501–509. [PubMed: 10548431]

12. Sainz B Jr, TenCate V, Uprichard SL. Three-dimensional Huh7 cell culture system for the study of Hepatitis C virus infection. Virol J. 2009; 6:103. [PubMed: 19604376]

13. Schadde E, Raptis DA, Schnitzbauer AA, Ardiles V, Tschuor C, Lesurtel M, et al. Prediction of Mortality After ALPPS Stage-1: An Analysis of 320 Patients From the International ALPPS Registry. Ann Surg. 2015; 262:780–785. discussion 5–6. [PubMed: 26583666]

14. Hughes RD, Mitry RR, Dhawan A. Current status of hepatocyte transplantation. Transplantation. 2012; 93:342–347. [PubMed: 22082820]

15. Szot GL, Koudria P, Bluestone JA. Transplantation of pancreatic islets into the kidney capsule of diabetic mice. Journal of visualized experiments : JoVE. 2007:404. [PubMed: 18989445]

16. Geerts A. History, heterogeneity, developmental biology, and functions of quiescent hepatic stellate cells. Seminars in liver disease. 2001; 21:311–335. [PubMed: 11586463]

17. Taub R. Liver regeneration: from myth to mechanism. Nature reviews Molecular cell biology. 2004; 5:836–847. [PubMed: 15459664]

18. Iredale JP. Models of liver fibrosis: exploring the dynamic nature of inflammation and repair in a solid organ. J Clin Invest. 2007; 117:539–548. [PubMed: 17332881]

19. Friedman SL. Hepatic stellate cells: protean, multifunctional, and enigmatic cells of the liver. Physiol Rev. 2008; 88:125–172. [PubMed: 18195085]

20. Gressner AM, Lahme B, Brenzel A. Molecular dissection of the mitogenic effect of hepatocytes on cultured hepatic stellate cells. Hepatology. 1995; 22:1507–1518. [PubMed: 7590670]

21. Uyama N, Shimahara Y, Kawada N, Seki S, Okuyama H, Iimuro Y, et al. Regulation of cultured rat hepatocyte proliferation by stellate cells. J Hepatol. 2002; 36:590–599. [PubMed: 11983441]

22. Abu-Absi SF, Hansen LK, Hu WS. Three-dimensional co-culture of hepatocytes and stellate cells. Cytotechnology. 2004; 45:125–140. [PubMed: 19003250]

23. Kasuya J, Sudo R, Mitaka T, Ikeda M, Tanishita K. Hepatic stellate cell-mediated three-dimensional hepatocyte and endothelial cell triculture model. Tissue Eng Part A. 2011; 17:361–370. [PubMed: 20799907]

24. Krause P, Saghatolislam F, Koenig S, Unthan-Fechner K, Probst I. Maintaining hepatocyte differentiation in vitro through co-culture with hepatic stellate cells. In Vitro Cell Dev Biol Anim. 2009; 45:205–212. [PubMed: 19184253]

25. Wong SF, No da Y, Choi YY, Kim DS, Chung BG, Lee SH. Concave microwell based size-controllable hepatosphere as a three-dimensional liver tissue model. Biomaterials. 2011; 32:8087–8096. [PubMed: 21813175]

26. Karatzas T, Neri AA, Baibaki ME, Dontas IA. Rodent models of hepatic ischemia-reperfusion injury: time and percentage-related pathophysiological mechanisms. The Journal of surgical research. 2014; 191:399–412. [PubMed: 25033703]

27. Shah KA, Shurey S, Green CJ. Apoptosis after intestinal ischemia-reperfusion injury: a morphological study. Transplantation. 1997; 64:1393–1397. [PubMed: 9392300]

28. Gujral JS, Bucci TJ, Farhood A, Jaeschke H. Mechanism of cell death during warm hepatic ischemia-reperfusion in rats: apoptosis or necrosis? Hepatology. 2001; 33:397–405. [PubMed: 11172341]

29. Suyavaran A, Thirunavukkarasu C. Preconditioning methods in the management of hepatic ischemia reperfusion- induced injury: update on molecular and future perspectives. Hepatology research : the official journal of the Japan Society of Hepatology. 2016

30. Yamanaka K, Houben P, Bruns H, Schultze D, Hatano E, Schemmer P. A systematic review of pharmacological treatment options used to reduce ischemia reperfusion injury in rat liver transplantation. PloS one. 2014; 10:e0122214. [PubMed: 25919110]

31. Sheu EG, Wakatsuki K, Oakes S, Carroll MC, Moore FD Jr. Prevention of intestinal ischemia-reperfusion injury in humanized mice. Surgery. 2016; 160:436–442. [PubMed: 27086922]

32. Chan RK, Ding G, Verna N, Ibrahim S, Oakes S, Austen WG Jr, et al. IgM binding to injured tissue precedes complement activation during skeletal muscle ischemia-reperfusion. The Journal of surgical research. 2004; 122:29–35. [PubMed: 15522311]

Author Manuscript

Author Manuscript

Author Manuscript

Author Manuscript
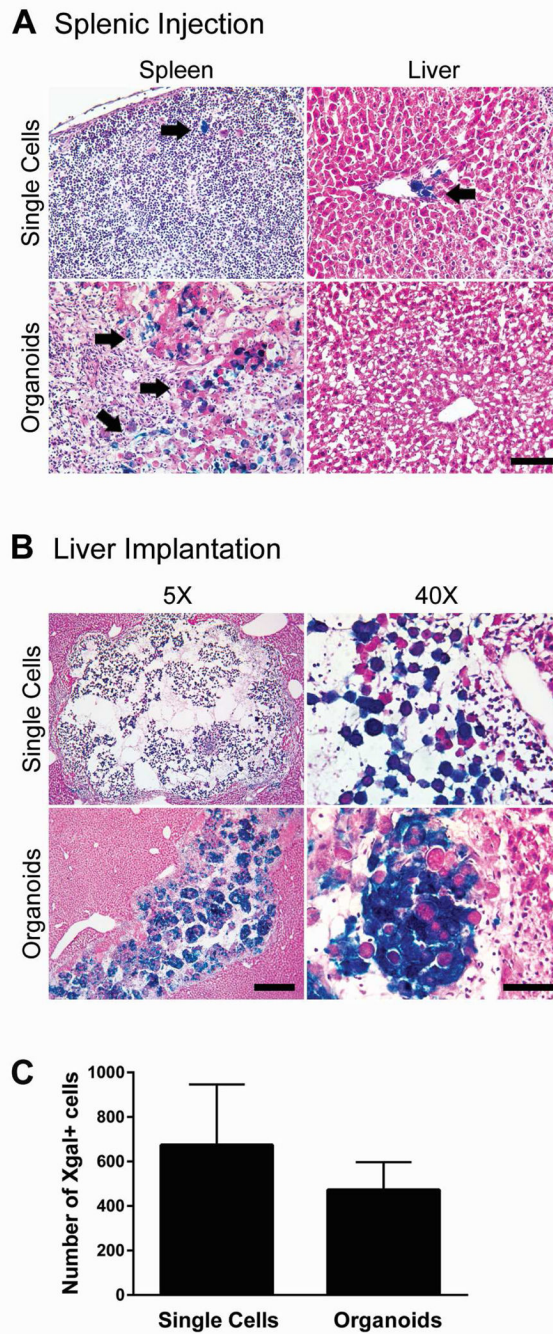
Figure 1.
Liver organoids injected through the spleen remain trapped within the spleen, whereas liver organoids orthotopically implanted directly into the liver parenchyma engraft locally within the implanted liver lobe. (A) Representative images of spleen and liver from recipient mice transplanted with Xgal+ single-cell hepatocytes or organoids by injection through the spleen. Splenic injection of single cells showed rare retention of Xgal+ hepatocytes in the spleen and low efficiency engraftment near portal veins within the liver parenchyma (arrows). Transplanted organoids remained trapped within the spleen (arrows). Magnification 5x.

Scale bar represents 400μm. (B) Representative images of livers that were directly implanted with single-cell hepatocytes or organoids. Implantation of either single cells or organoids showed local engraftment in the implanted liver lobe. Single cells were loosely dispersed within the hepatotomy site. Organoids retained their compact spheroid architecture. Scale bars represent 400μm (5x images) and 60μm (40x images). (C) Quantification of implanted hepatocytes by enumerating Xgal^{+} cells in single cell (n=9) versus organoid (n=6) orthotopic implantation. Error bars represent SEM.
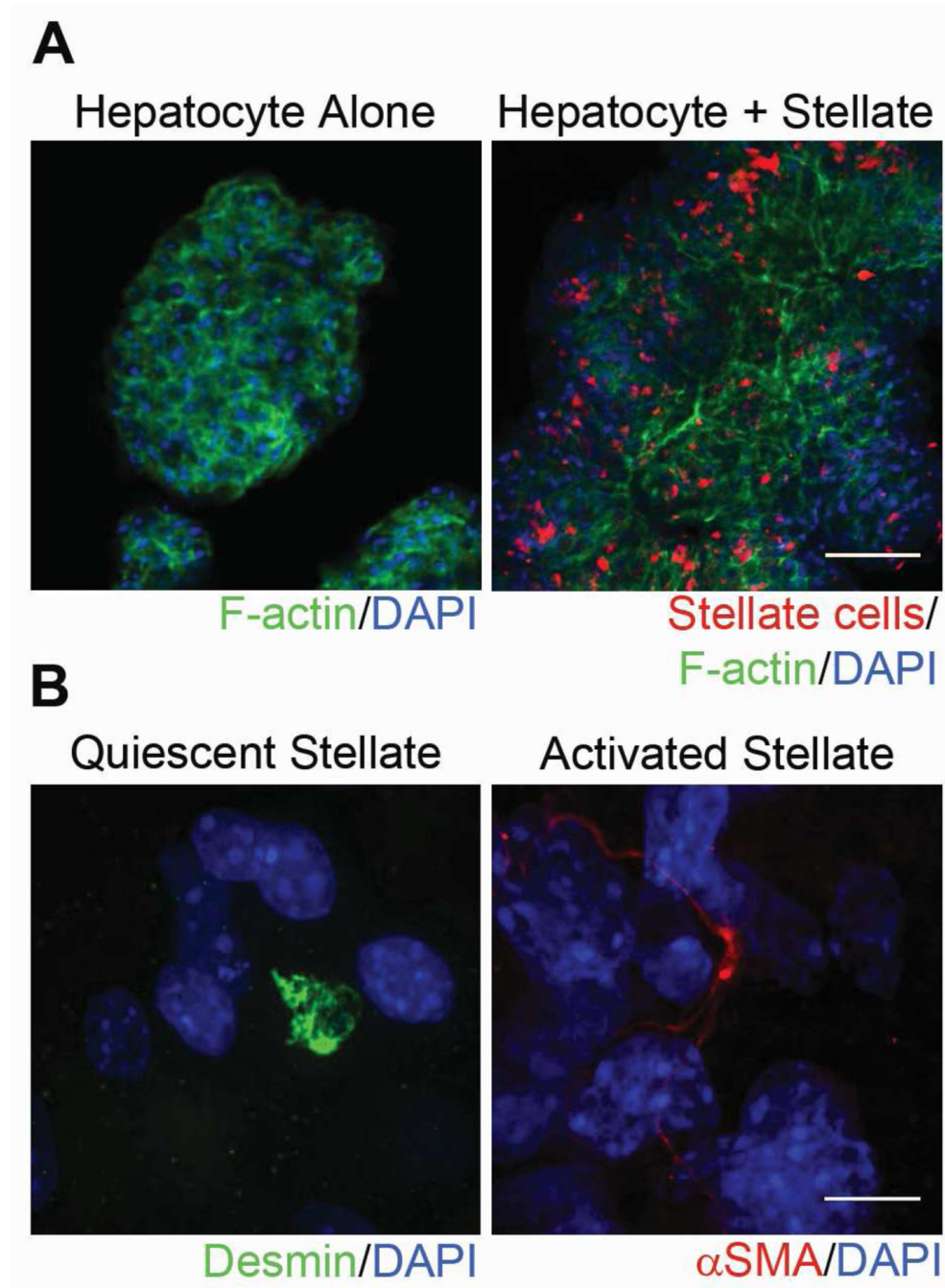
Figure 2.
Hepatocyte-stellate cell organoids demonstrate widespread distribution of stellate cells throughout the organoid and include both quiescent and activated stellate cells. (A) Representative confocal images of hepatocyte-alone and hepatocyte-stellate cell organoids. Organoids were stained with phalloidin to indicate F-actin (green) and DAPI to indicate nuclei (blue). Stellate cells were pretreated and identified with CellTracker CMTPX Red dye (red). Magnification 10x. Scale bar represents 100μm. (B) Representative confocal images of individual stellate cells within hepatocyte-stellate organoids show the presence of both
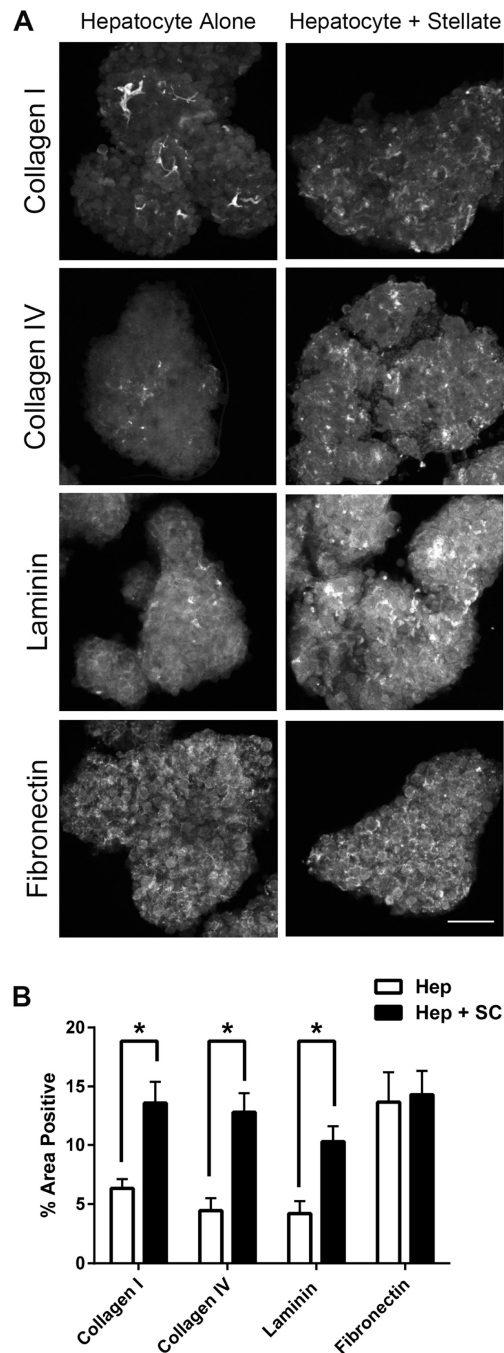
quiescent and activated states. Quiescent stellate cells were identified via desmin (green) and round cell shape, whereas activated stellate cells were marked by αSMA (red) and elongated cell shape. Nuclei were stained with DAPI (blue). Magnification 100x. Scale bar represents 10μm.

Figure 3.
Hepatocyte-stellate cell organoids show significant increases in several extracellular matrix (ECM) proteins compared to hepatocyte-alone organoids. (A) Representative confocal images of hepatocyte-stellate cell organoids demonstrated increased presence of collagen I, collagen IV, and laminin compared to hepatocyte-alone organoids, whereas levels of fibronectin were similar between the two organoid types. Magnification 10x. Scale bar represents 100μm. (B) Quantification of ECM components in hepatocyte-only (Hep) and hepatocyte-stellate (Hep + SC) organoids. Percent area positive for each ECM protein was
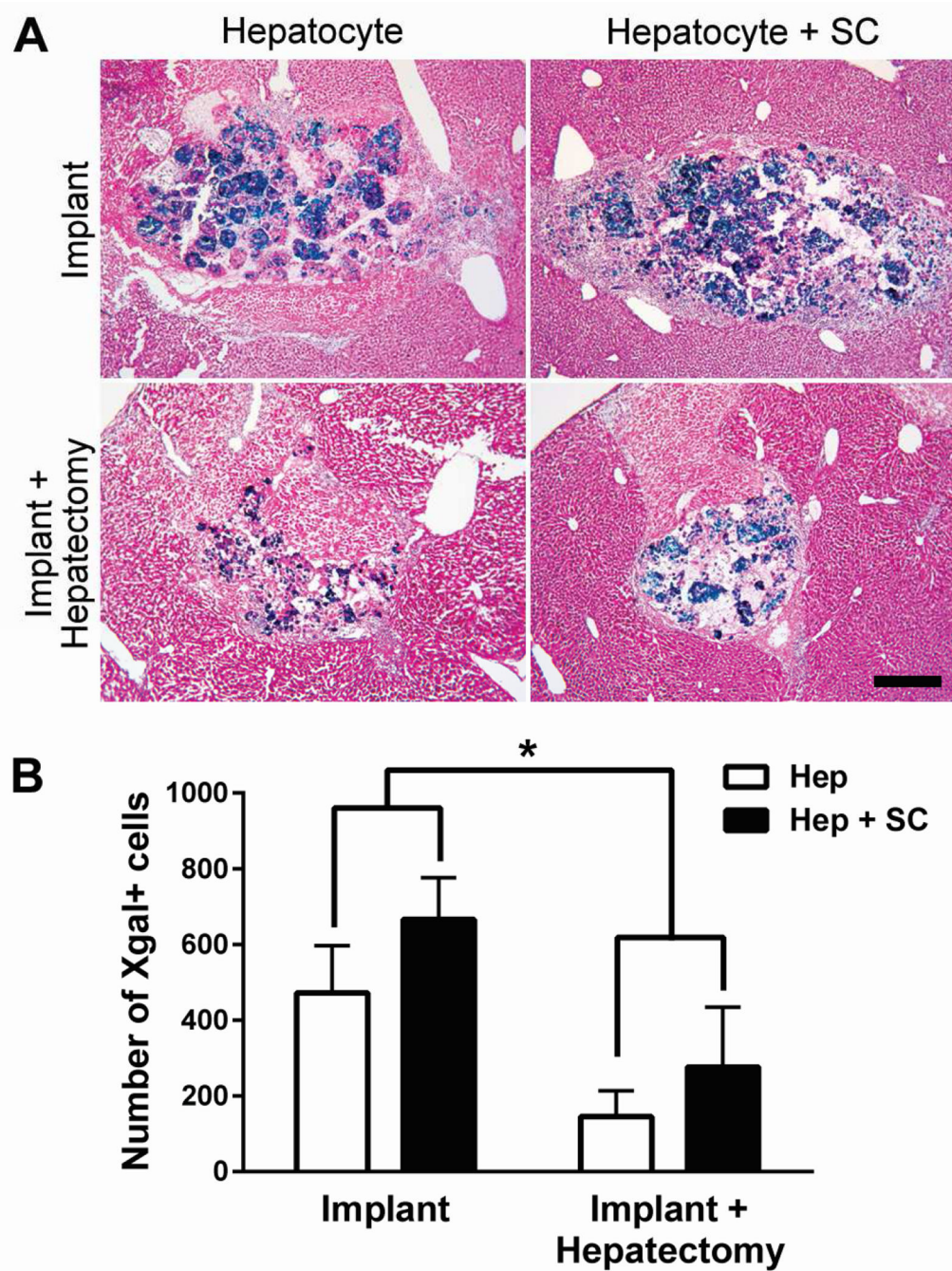
determined by digital imaging analysis in at least 10 individual organoids per ECM component per group. *p<0.05 by two-tailed Student's t-test. Error bars represent SEM.
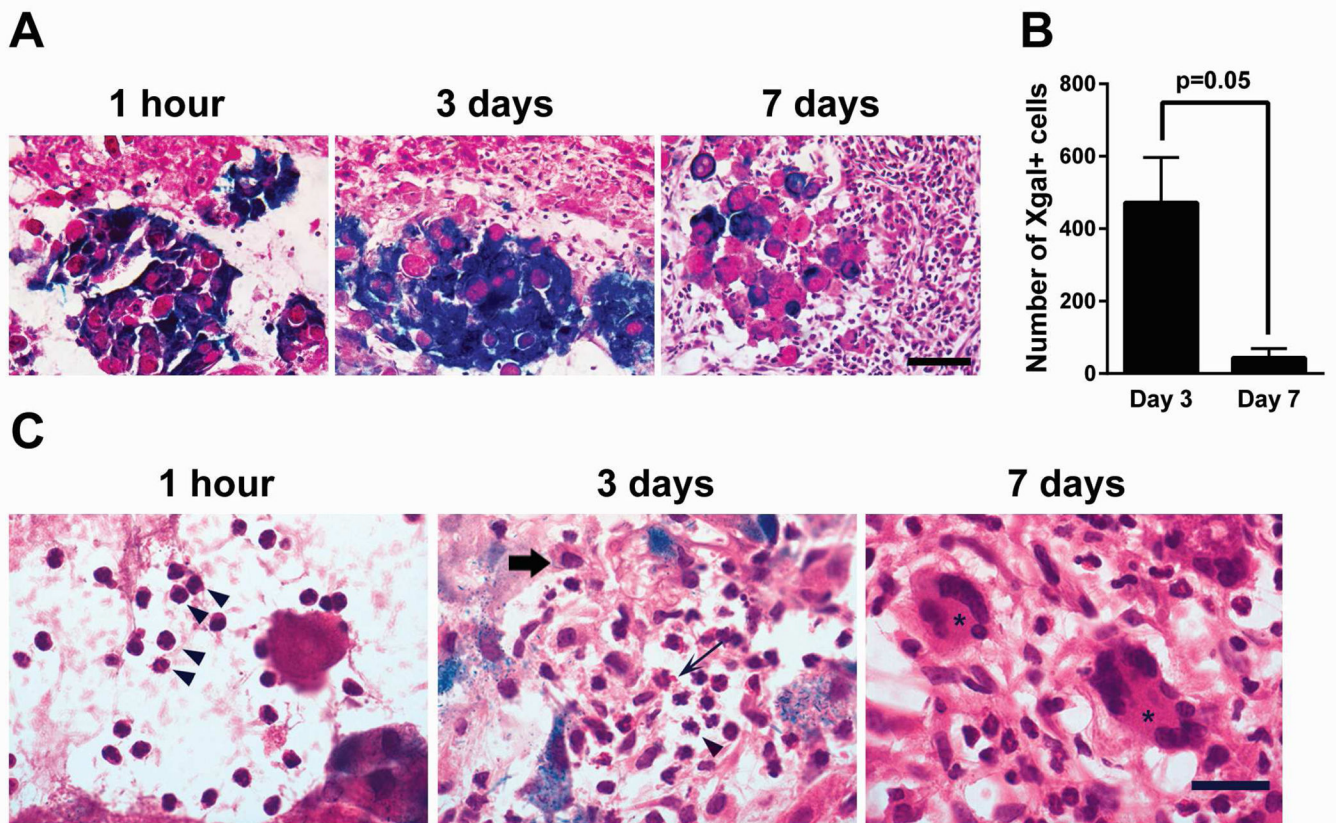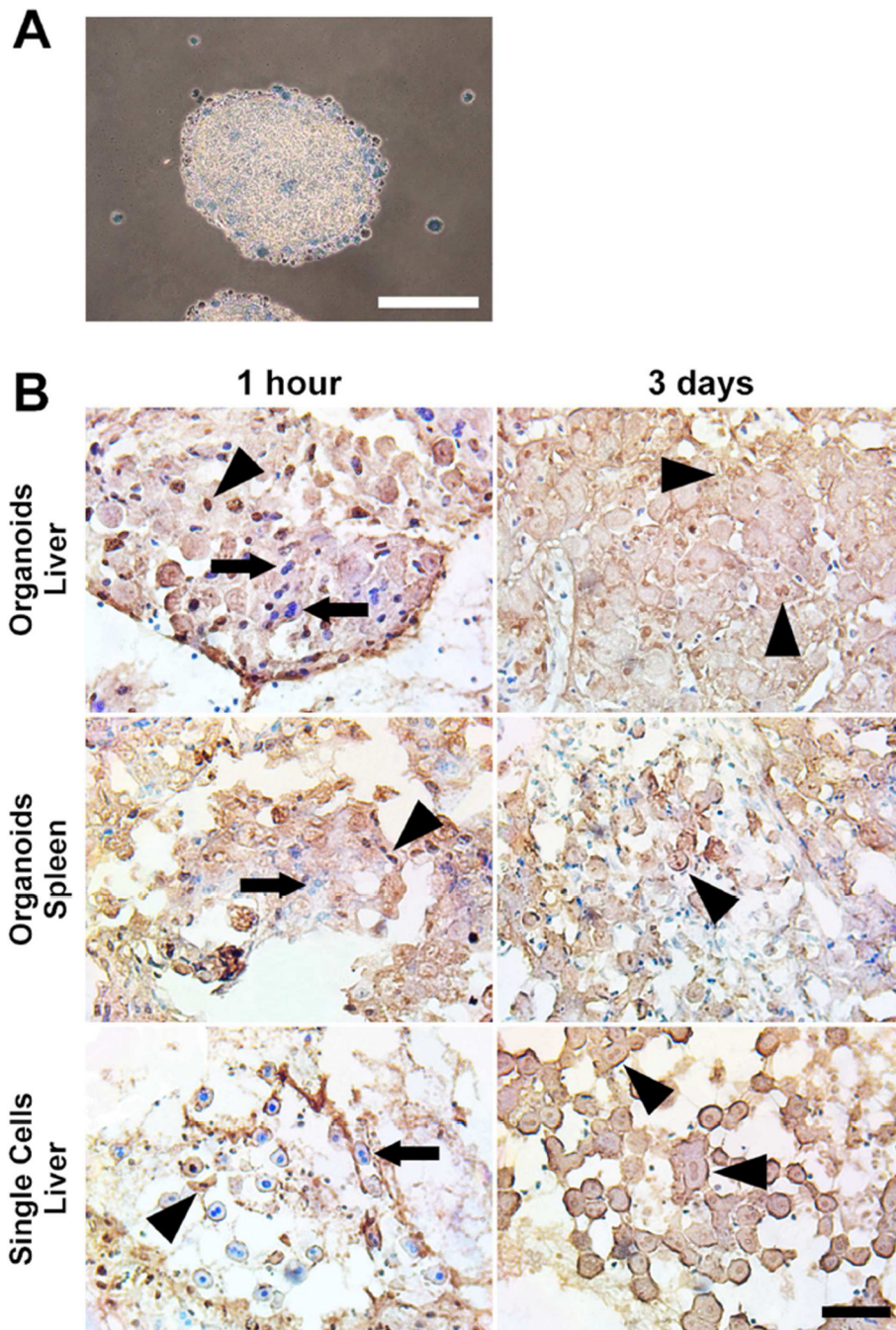
Figure 4.
Hepatocyte-stellate cell organoids show engraftment comparable to that of hepatocyte-alone organoids, whereas partial hepatectomy significantly reduces engraftment of both organoid types. (A) Representative images of liver sections demonstrating implantation outcomes of hepatocyte-alone (Hep) organoids with (n=9) and without (n=6) partial hepatectomy, in comparison with hepatocyte-stellate cell (Hep + SC) organoids with (n=3) and without (n=3) partial hepatectomy. Images are representative of at least 6 sections evaluated per mouse. Magnification 5x. Scale bar represents 400μm. (B) Quantification of implanted hepatocytes

by enumerating Xgal$^+$ cells through digital image analysis. *p<0.01 by two-way ANOVA. Two-way ANOVA analysis showed no significant interaction (p = 0.79) between the type of surgery (with or without hepatectomy) and the type of organoid (with or without stellate cells). The p-values for the type of surgery and the type of organoid are 0.008 and 0.19, respectively. Error bars represent SEM.

Figure 5.
Inflammatory cells surrounding implanted organoids accumulate over time, starting with a predominantly neutrophilic infiltration and evolving into a chronic inflammatory reaction with multinucleated giant cells. (A) Representative images of host inflammatory response and hepatocyte organoids in liver sections at 1 hour (n=3), 3 days (n=6), and 7 days (n=7) after organoid implantation. Images are representative of at least 4 sections evaluated per mouse. Magnification 40x. Scale bar represents 60μm. (B) Time course of Xgal$^+$ cells detected at organoid implantation sites comparing 3 days (n=6) and 7 days (n=7) after implantation. p=0.05 by two-tailed Student's t-test. Error bars represent SEM. (C) High-powered morphological analysis of the inflammatory infiltrates demonstrated the presence of predominantly neutrophils (arrowheads) at 1 hour after implantation. By 3 days, the expanded inflammatory infiltrate included recruitment of neutrophils (arrowhead), eosinophils (thin arrow), and macrophages (thick arrow). By 7 days, a chronic inflammatory reaction had developed with numerous multinucleated giant cells (asterisk). Magnification 60x. Scale bar represents 20μm.

Figure 6.
Hepatocytes within viable organoids implanted into the liver parenchyma show early apopotosis and become necrotic by 3 days. (A) Hepatocyte organoids prior to implantation are viable and exclude trypan blue. Hepatocytes that remain as single cells in 3D culture are dead and trypan blue positive. Scale bar represents 200μm. (B) Hepatocyte organoids or freshly isolated single-cell hepatocytes were implanted into the liver or spleen. At 1 hour and 3 days post-implantation, TUNEL staining was performed to detect apoptotic nuclei (brown nuclei, indicated by arrowheads), and counterstained with methyl green for viable nuclei

(blue nuclei, indicated by arrows). By 3 days after implantation, most hepatocytes were anucleated with washed-out cytoplasm, consistent morphologically with necrosis. Scale bar represents 100μm.